Robust generation of entanglement in Bose-Einstein condensates by collective atomic recoil

Mary M. Cola, Matteo G. A. Paris, and Nicola Piovella

Dipartimento di Fisica dell'Università di Milano and INFN and INFM at Università di Milano, Via Celoria 16, Milano I-20133, Italy
(Received 7 April 2004; published 13 October 2004)

We address the dynamics induced by collective atomic recoil in a Bose-Einstein condensate in the presence of radiation losses and atomic decoherence. In particular, we focus on the linear regime of the lasing mechanism, and analyze the effects of losses and decoherence on the generation of entanglement. The dynamics is that of three bosons, two atomic modes interacting with a single-mode radiation field, coupled with a bath of oscillators. The resulting three-mode dissipative Master equation is solved analytically in terms of the Wigner function. We examine in details the two complementary limits of *high-Q cavity* and *bad cavity*, the latter corresponding to the so-called superradiant regime, both in the quasiclassical and quantum regimes. We found that three-mode entanglement as well as two-mode atom-atom and atom-radiation entanglement is generally robust against losses and decoherence, thus making the present system a good candidate for the experimental observation of entanglement in condensate systems. In particular, steady-state entanglement may be obtained both between atoms with opposite momenta and between atoms and photons.

I. INTRODUCTION

The experimental realization of Bose-Einstein condensation opened the possibility to generate macroscopic atomic fields whose quantum statistical properties can in principle be manipulated and controlled [1]. The system considered here for this purpose is an elongated Bose-Einstein condensate (BEC) driven by a far off-resonant pump laser of wave vector $k_p = \omega_p / c$ along the condensate long axis and coupled to a single mode in an optical ring cavity. The mechanism at the basis of this kind of physics is the so-called collective atomic recoil lasing (CARL) [2] in its full quantized version [3–6]. In CARL the scattered radiation mode and the atomic momentum side modes become macroscopically occupied via a collective instability. A peculiar aspect of the quantum regime is the possibility of populating single momentum modes separated by $\Delta p = 2\hbar k_p$ off the condensate ground state with zero initial momentum. The experimental observation of CARL in a BEC has been until now realized in the so-called superradiant regime [7–9], i.e., without the optical cavity. In this case the radiation is emitted along the "end-fire modes" of the condensate [10] with very large radiation losses (in the mean field model, with $2\kappa \approx c/L$, where 2κ is the radiation intensity decay rate and L is the condensate length). Recent experiments reported in [11] represent a realization of CARL in a ring cavity for a noncondensate sample of cold atoms. The apparatus is very promising and makes it likely that CARL experiments with BECs in an optical cavity will be performed in the near future.

Recent works have shown that atom-atom or atom-photon entanglement and squeezing [6,12,13] can be produced in the linear regime of CARL, in which the ground state of the condensate remains approximately undepleted. In this regime, the atomic multimode system can be described by only two momentum side modes, with $p = \pm 2\hbar k_p$. Furthermore, this source of entanglement has been also proposed for a quantum teleportation scheme among atoms and photons [14].

The results presented in [6,12,13] refer to the ideal case of a perfect optical cavity and an atomic system free of deco-

herence. However, in view of an experimental observation of entanglement, a detailed analysis of the sources of noise is in order, which in turn may be a serious limitation for entanglement in CARL [15]. Also, it has not yet been proved that BEC superradiance experiments may generate entangled atom-photon states, as it has been conjectured in [10]. This issue is investigated in this paper, where we demonstrate the entangled properties of the atom-atom and atom-photon pairs produced in the linear stage of the superradiant CARL regime in a BEC.

The aim of the present work is to analyze systematically, by solving the three-mode Master equation in the Wigner representation, the effects of losses and decoherence on the generation of entanglement. We will investigate the effects of either a small atomic decoherence or a finite mirror transmission of the optical cavity, and then analyze in details the generation of entanglement in the superradiant regime, where the cavity losses are important.

The paper is structured as follows. In Sec. II we briefly review the ideal dynamics and derive the general solution of the Master equation. In Sec. III we consider the evolution of the system starting from the vacuum and calculate the relevant expectation values, such as average and variance of the occupation number and two-mode squeezing parameters. In Sec. IV the different working regimes are introduced and the dynamics analyzed, whereas in Sec. V we investigate three- and two-mode entanglement properties of the system as a function of loss and decoherence parameters. Section VI closes the paper with some concluding remarks.

II. DISSIPATIVE MASTER EQUATION

We consider a one-dimensional (1D) geometry in which an off-resonant laser pulse, with Rabi frequency $\Omega_0 = dE_0/\hbar$ (where d is the dipole matrix element and E_0 is the electric field amplitude) and detuned from the atomic resonance by $\Delta_0 = \omega_p - \omega_0$, is injected in a ring cavity aligned with the symmetry z axis of an elongated BEC. The dimensionless posi-

tion and momentum of the atom along the axis $\hat{z}$ are $\theta = 2k_p z$ and $p = p_z/2\hbar k_p$. The interaction time is $\tau = \rho \omega_r t$, where $\omega_r = 2\hbar k_p^2/m$ is the recoil frequency, m is the atomic mass, $\rho = (\Omega_0/2\Delta_0)^{2/3}(\omega_p d^2 N/V\hbar \epsilon_0 \omega_r^2)^{1/3}$ is the CARL parameter, N is the number of atoms in the cavity mode volume V and ϵ_0 is the permittivity of the free space.

In a second quantized model for CARL [5,6] the atomic field operator $\hat{\Psi}(\theta)$ obeys the bosonic equal-time commutation relations $[\hat{\Psi}(\theta),\hat{\Psi}^\dagger(\theta')] = \delta(\theta - \theta')$, $[\hat{\Psi}(\theta),\hat{\Psi}(\theta')] = 0$, and the normalization condition is $\int_0^{2\pi} d\theta \hat{\Psi}(\theta)^\dagger \hat{\Psi}(\theta) = N$. We assume that the atoms are delocalized inside the condensate and that, at zero temperature, the momentum uncertainty σ_{p_z} can be neglected with respect to $2\hbar k_p$

In this limit, we can introduce creation and annihilation operators for an atom with a definite momentum p, i.e., $\hat{\Psi}(\theta) = \Sigma_m \hat{c}_m \langle \theta | m \rangle$, where $p|m\rangle = m|m\rangle$ (with $m = -\infty, \ldots, \infty$), $\langle \theta | m \rangle = (1/\sqrt{2\pi})\exp(im\theta)$ and $\hat{c}_m$ are bosonic operators obeying the commutation relations $[\hat{c}_m,\hat{c}_n^\dagger] = \delta_{mn}$ and $[\hat{c}_m,\hat{c}_n] = 0$. The Hamiltonian in this case is [6]

$$\hat{H} = \sum_{n=-\infty}^{\infty} \left\{ \frac{n^2}{\rho}\hat{c}_n^\dagger \hat{c}_n + i\sqrt{\frac{\rho}{2N}}(\hat{a}^\dagger \hat{c}_n^\dagger \hat{c}_{n+1} - \text{H.c.}) \right\} - \delta \hat{a}^\dagger \hat{a},$$

$$(1)$$

where $\hat{a}$ is the annihilation operator (with $[\hat{a},\hat{a}^\dagger] = 1$) for the cavity mode (propagating along the positive direction of the z axis) with frequency ω_s and $\delta = (\omega_p - \omega_s)/\rho\omega_r$ is the detuning with respect to the pump frequency ω_p. Let us now consider the equilibrium state with no photons and all the atoms at rest, i.e., with $|\Psi_0\rangle = \sqrt{N}|0\rangle$. Linearizing around this equilibrium state and defining the operators $\hat{a}_1 = \hat{c}_{-1}e^{i\delta\tau}$, $\hat{a}_2 = \hat{c}_1 e^{-i\delta\tau}$, and $\hat{a}_3 = \hat{a}e^{-i\delta\tau}$, the Hamiltonian (1) reduces to that for three parametrically coupled harmonic oscillator operators [3,12,13]:

$$\hat{H} = \delta_+ \hat{a}_2^\dagger \hat{a}_2 - \delta_- \hat{a}_1^\dagger \hat{a}_1 + i\sqrt{\frac{\varrho}{2}}[(\hat{a}_1^\dagger + \hat{a}_2)\hat{a}_3^\dagger - (\hat{a}_1 + \hat{a}_2^\dagger)\hat{a}_3],$$

$$(2)$$

where $\delta_\pm = \delta \pm 1/\rho$. In Ref. [6] we have explicitly evaluated the state evolved from the vacuum of the three modes, $|0_1, 0_2, 0_3\rangle$, as

$$|\psi(\tau)\rangle = \frac{1}{\sqrt{1 + \langle \hat{n}_1 \rangle}} \sum_{n,m=0}^{\infty} \left(\frac{\langle \hat{n}_3 \rangle}{1 + \langle \hat{n}_1 \rangle} \right)^{m/2} \left(\frac{\langle \hat{n}_2 \rangle}{1 + \langle \hat{n}_1 \rangle} \right)^{n/2}$$

$$\times e^{-i(n\phi_2 + m\phi_3)} \sqrt{\frac{(m+n)!}{m!\,n!}} |m+n,n,m\rangle, \quad (3)$$

where $\langle \hat{n}_i \rangle = \langle \hat{a}_i^\dagger \hat{a}_i \rangle$ with $i = 1,2,3$ are the expectation values of the occupation numbers of the three modes, related by the constant of motion $\hat{C} = \hat{n}_1 - \hat{n}_2 - \hat{n}_3$. In this paper we extend our previous analysis to include the effects of atomic decoherence and cavity radiation losses. In this case the dynamics of the system is described by the following Master equation:

$$\frac{d\hat{\varrho}}{d\tau} = -i[\hat{H},\hat{\varrho}] + 2\gamma_1 L[\hat{a}_1]\hat{\varrho} + 2\gamma_2 L[\hat{a}_2]\hat{\varrho} + 2\kappa L[\hat{a}_3]\hat{\varrho},$$

$$(4)$$

where γ_1, γ_2, and κ are the damping rates for the modes a_i and $L[\hat{a}_i]$ is the Lindblad superoperator

$$L[\hat{a}_i]\hat{\varrho} = \hat{a}_i \hat{\varrho} \hat{a}_i^\dagger - \frac{1}{2}\hat{a}_i^\dagger \hat{a}_i \hat{\varrho} - \frac{1}{2}\hat{\varrho}\hat{a}_i^\dagger \hat{a}_i.$$

$$(5)$$

The atomic decay stems from coherence loss between the undepleted ground state with $p_z = 0$ and the side modes with $p_z = \pm 2\hbar k_p$. In general, we assume that the two atomic modes may have different decoherence rates, depending on the direction of recoil [9]. The radiation decay constant is $\kappa = cT/2\mathcal{L}$, where T is the transmission of the cavity and $\mathcal{L}$ is the cavity length. Through a standard procedure [16], the Master equation can be transformed into a Fokker-Planck equation for the Wigner function of the state $\hat{\varrho}$,

$$W(\alpha_1,\alpha_2,\alpha_3,\tau) = \int \prod_{i=1}^{3} \frac{d^2\xi_i}{\pi^2} e^{\xi_i^* \alpha_i - \alpha_i^* \xi_i} \chi(\xi_1,\xi_2,\xi_3,\tau), \quad (6)$$

where α_j and ξ_j are complex numbers and χ is the characteristic function defined as

$$\chi(\xi_1,\xi_2,\xi_3,\tau) = \text{Tr}[\hat{\varrho}(\tau)\hat{D}_1(\xi_1)\hat{D}_2(\xi_2)\hat{D}_3(\xi_3)], \quad (7)$$

where $\hat{D}_j(\xi_j) = \exp(\xi_j \hat{a}_j^\dagger - \xi_j^* \hat{a}_j)$ is a displacement operator for the jth mode. Using the differential representation of the Lindblad superoperator, the Fokker-Planck equation is

$$\frac{\partial W}{\partial \tau} = -(\mathbf{u}'^T \mathbf{A}\mathbf{u} + \text{c.c.})W + \mathbf{u}'^T \mathbf{D}\mathbf{u}'^* W, \quad (8)$$

where

$$\mathbf{u}^T = (\alpha_1^*, \alpha_2, \alpha_3), \quad \mathbf{u}'^T = \left(\frac{\partial}{\partial \alpha_1^*}, \frac{\partial}{\partial \alpha_2}, \frac{\partial}{\partial \alpha_3} \right) \quad (9)$$

and $\mathbf{A}$ and $\mathbf{D}$ are the following drift and diffusion matrices:

$$\mathbf{A} = \begin{pmatrix} \gamma_1 + i\delta_- & 0 & -\sqrt{\rho/2} \\ 0 & \gamma_2 + i\delta_+ & \sqrt{\rho/2} \\ -\sqrt{\rho/2} & -\sqrt{\rho/2} & \kappa \end{pmatrix},$$

$$\mathbf{D} = \begin{pmatrix} \gamma_1 & 0 & 0 \\ 0 & \gamma_2 & 0 \\ 0 & 0 & \kappa \end{pmatrix}. \quad (10)$$

The solution of the Fokker-Planck equation (8) reads as follows:

$$W(\mathbf{u},\tau) = \int d^2\mathbf{u}_0 W(\mathbf{u}_0,0)G(\mathbf{u},\tau;\mathbf{u}_0,0), \quad (11)$$

where $W(\mathbf{u}_0,0)$ is the Wigner function for the initial state and the Green function $G(\mathbf{u},t;\mathbf{u}_0,0)$ is the solution of Eq. (8) for the initial condition $G(\mathbf{u},0;\mathbf{u}_0,0) = \delta^{(3)}(\mathbf{u} - \mathbf{u}_0)$. The calculation of the Green function, the solution of Eq. (8), is reported in detail in Appendix A and yields the following result:

$$G(\mathbf{u}, \tau; \mathbf{u}_0, 0) = \frac{1}{\pi^3 \det \mathbf{Q}(\tau)} \exp\{-[\mathbf{u} - \mathbf{M}(\tau)\mathbf{u}_0]^\dagger \mathbf{Q}^{-1}(\tau)$$
$$\times [\mathbf{u} - \mathbf{M}(\tau)\mathbf{u}_0]\}, \qquad (12)$$

where

$$\mathbf{M}(\tau) \equiv e^{\mathbf{A}\tau} = \begin{pmatrix} f_{11}(\tau) & f_{12}(\tau) & f_{13}(\tau) \\ -f_{12}(\tau) & f_{22}(\tau) & f_{23}(\tau) \\ f_{13}(\tau) & -f_{23}(\tau) & f_{33}(\tau) \end{pmatrix} \qquad (13)$$

and

$$\mathbf{Q}(\tau) = \int_0^\tau d\tau' \mathbf{M}(\tau') \mathbf{D} \mathbf{M}^\dagger(\tau'). \qquad (14)$$

In Eq. (13) the complex functions f_{ij}, given explicitly in Appendix B, are the sum of three terms proportional to $e^{i\omega_k\tau}$, where ω_k, with $k = 1, 2, 3$, are the three roots of the cubic equation:

$$[\omega - \delta - i(\kappa - \gamma_+)]\left[\omega^2 - \left(\frac{1}{\rho} + i\gamma_-\right)^2\right] + 1 + i\rho\gamma_- = 0 \qquad (15)$$

and $\gamma_\pm = (\gamma_1 \pm \gamma_2)/2$

III. EVOLUTION FROM VACUUM AND EXPECTATION VALUES

Let us now assume that the initial state is the vacuum. The characteristic function and the Wigner function at $\tau = 0$ are given by

$$\chi(\boldsymbol{\xi}, 0) = \exp\{-\boldsymbol{\xi}^\dagger \mathbf{C}_0 \boldsymbol{\xi}\}, \quad W(\mathbf{u}, 0) = \left(\frac{2}{\pi}\right)^3 \exp\{-\mathbf{u}^\dagger \mathbf{C}_0^{-1} \mathbf{u}\}, \qquad (16)$$

where $\boldsymbol{\xi} = (\xi_1^*, \xi_2, \xi_3)$ and the covariance matrix is multiple of the identity matrix $\mathbf{C}_0 = \frac{1}{2}\mathbf{I}$. Since the initial state is Gaussian and the convolution in Eq. (11) maintains this character we have that the Wigner function is Gaussian at any time τ,

$$W(\mathbf{u}, \tau) = \frac{1}{\pi^3 \sqrt{\det \mathbf{C}(\tau)}} \exp\{-\mathbf{u}^\dagger \mathbf{C}(\tau)^{-1} \mathbf{u}\}. \qquad (17)$$

After some algebra, we found that the covariance matrix is given by

$$\mathbf{C}(\tau) = \mathbf{Q}(\tau) + \frac{1}{2}\mathbf{M}(\tau)\mathbf{M}^\dagger(\tau), \qquad (18)$$

where the explicit form of the elements $C_{ij} = \langle(u_i - \langle u \rangle_i)(u_j - \langle u \rangle_j)^*\rangle$ in terms of the functions f_{ij} is reported in Appendix B. Since the state is Gaussian, from Eq. (18) it is possible to derive all the expectation values for the three modes. In particular, $C_{ii} = 1/2 + \langle \hat{n}_i \rangle$, $C_{12} = \langle \hat{a}_1^\dagger \hat{a}_2^\dagger \rangle$, $C_{13} = \langle \hat{a}_1^\dagger \hat{a}_3^\dagger \rangle$, and $C_{23} = \langle \hat{a}_2 \hat{a}_3^\dagger \rangle$. The number variances and the equal-time correlation functions for the mode numbers are calculated from the fourth-order covariance matrix $G_{ijkl} = \langle(u_i - \langle u \rangle_i)(u_j - \langle u \rangle_j)(u_k - \langle u \rangle_k)^*(u_l - \langle u \rangle_l)^*\rangle$, which in turn is related to the covariance matrix as follows:

$$G_{ijkl} = C_{ki}C_{lj} + C_{li}C_{kj}. \qquad (19)$$

In particular, we have

$$G_{iiii} = \langle \hat{n}_i^2 \rangle + \langle \hat{n}_i \rangle + \frac{1}{2}, \qquad (20)$$

$$G_{ijij} = \langle \hat{n}_i \hat{n}_j \rangle + \frac{1}{2}\langle \hat{n}_i \rangle + \frac{1}{2}\langle \hat{n}_j \rangle + \frac{1}{4} \quad (i \neq j). \qquad (21)$$

From Eqs. (19)–(21) it follows that

$$\sigma^2(n_i) = \langle \hat{n}_i \rangle (\langle \hat{n}_i \rangle + 1), \qquad (22)$$

$$g_i^{(2)} = \frac{\langle \hat{a}_i^\dagger \hat{a}_i^\dagger \hat{a}_i \hat{a}_i \rangle}{\langle \hat{n}_i \rangle^2} = 2, \qquad (23)$$

$$g_{i,j}^{(2)} = \frac{\langle \hat{n}_i \hat{n}_j \rangle}{\langle \hat{n}_i \rangle \langle \hat{n}_j \rangle} = 1 + \frac{|C_{ij}|^2}{\langle \hat{n}_i \rangle \langle \hat{n}_j \rangle}, \qquad (24)$$

where $\sigma^2(n_i) = \langle \hat{n}_i^2 \rangle - \langle \hat{n}_i \rangle^2$, with $i = 1, 2, 3$, and $i \neq j$ in Eq. (24). The two-mode number squeezing parameter is calculated as [12]

$$\xi_{i,j} = \frac{\sigma^2(\hat{n}_i - \hat{n}_j)}{\langle \hat{n}_i \rangle + \langle \hat{n}_j \rangle} = \frac{\sigma^2(n_i) + \sigma^2(n_j) - 2|C_{ij}|^2}{\langle \hat{n}_i \rangle + \langle \hat{n}_j \rangle}. \qquad (25)$$

We observe, from Eqs. (22) and (23) that the statistics is that of a chaotic (i.e., thermal) state, as obtained in Ref. [6] for the lossless case. If the two modes are perfectly number-squeezed, then $\xi_{i,j} = 0$, whereas if they are independent and coherent, $\xi_{i,j} = 1$. As it will be clear in the following sections, it is also worth to introduce also the atomic density operator for the linearized matter-wave field $\hat{\Psi}(\theta) \approx [\sqrt{N} + a_1 e^{-i(\theta + \delta\tau)} + a_2 e^{i(\theta + \delta\tau)}]/\sqrt{2\pi}$, defined as

$$\hat{n}(\theta) = \hat{\Psi}^\dagger(\theta)\hat{\Psi}(\theta) \approx \frac{N}{2\pi}(1 + \hat{B}e^{-i(\theta + \delta\tau)} + \hat{B}^\dagger e^{i(\theta + \delta\tau)}), \qquad (26)$$

where $\hat{B} = (a_1^\dagger + a_2)/\sqrt{N}$ is the bunching operator, with $\langle \hat{B} \rangle = 0$ and

$$\langle \hat{B}^\dagger \hat{B} \rangle = \frac{1}{N}(C_{11} + C_{22} + C_{12} + C_{21}). \qquad (27)$$

The non-Hermitian operator $\hat{B}$ describes amplitude and phase evolution of the matter-wave grating with a periodicity of half of the laser wavelength [3]

IV. ANALYSIS OF WORKING REGIMES

We now investigate the different regimes of operation of CARL. For the sake of simplicity, we will discuss only the case with $\gamma_1 = \gamma_2 = \gamma$, so that $\gamma_+ = \gamma$ and $\gamma_- = 0$. In this case the cubic equation (15) becomes

$$[\omega - \delta - i(\kappa - \gamma)]\left(\omega^2 - \frac{1}{\rho^2}\right) + 1 = 0. \qquad (28)$$

We will discuss two pairs of different regimes for CARL, as defined in Ref. [17], i.e., (i) the semiclassical good-cavity
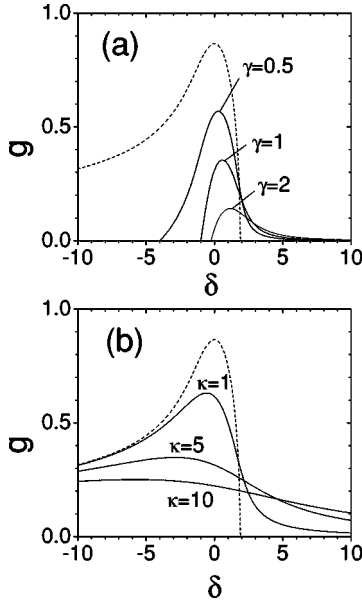
FIG. 1. Growth rate $g=-\text{Im}\,\omega-\gamma$ vs δ for the unstable root of the cubic equation (15) in the semiclassical limit, $\rho=100$. In (a) $\kappa=0$, and $\gamma=0.5,1,2$; in (b) $\gamma=0$ and $\kappa=1,5,10$. The dashed lines represent the case $\kappa=\gamma=0$.
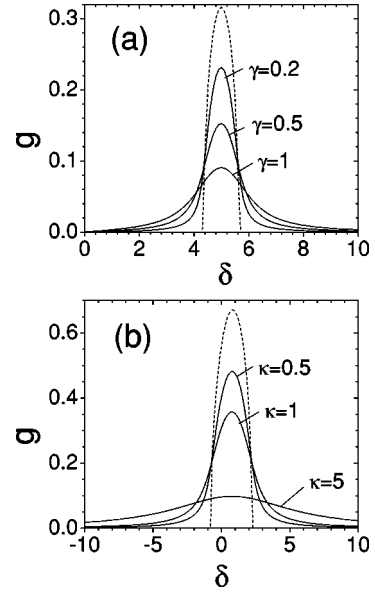

FIG. 2. Growth rate $g=-\text{Im}\,\omega-\gamma$ vs δ for the unstable root of the cubic equation (15) in the quantum limit. In (a) $\rho=0.2$, $\kappa=0$, and $\gamma=0.2,0.5,1$; in (b) $\rho=1$, $\gamma=0$, and $\kappa=0.5,1,5$. The dashed lines represent the case $\kappa=\gamma=0$.

regime ($\rho\gg1$ and $\kappa\ll1$); (ii) the quantum good-cavity regime ($\kappa^2\ll\rho<1$); (iii) the semiclassical superradiant regime ($\rho\gg\sqrt{2\kappa}>1$); (iv) the quantum superradiant regime ($\kappa^2\gg\sqrt{2\kappa}>\rho$). Also, we note that the case $\gamma=\kappa$ is worth special attention. In fact, in this case Eq. (28) is independent on losses: the effect of decoherence is only a overall factor $\exp(-\gamma\tau)$ multiplying the functions f_{ij}, elements of the matrix **M**. Hence, it is expected that the case $\gamma=\kappa$ will have statistical properties similar to those of the ideal case without losses, as it will be discussed below.

A. CARL instability

First, we investigate the effect of decoherence and cavity losses on the CARL instability in the different regimes. For large values of τ the functions f_{ij} of Eq. (13) grow as $\exp(g\tau)$, where $g=-\text{Im}\,\omega-\gamma$ and ω is the unstable root of Eq. (28) with a negative imaginary part. The exponential rate g is a gain when it is positive or a loss when it is negative.

In Fig. 1 we plot g vs δ in the semiclassical regime (e.g., $\rho=100$) for the good-cavity case ($\kappa=0$) and $\gamma=0.5,1,2$ [Fig. 1(a)], whereas the transition to the superradiant regime is shown in Fig. 1(b) for $\kappa=1,5,10$ and $\gamma=0$. The dashed line in Fig. 1 shows the gain $g^{(0)}$ for the ideal case $\kappa=\gamma=0$. A similar behavior is obtained in the quantum regime shown in Fig. 2, where g is plotted vs δ for $\rho=0.2$, $\kappa=0$, and $\gamma=0.2,0.5,1$ [Fig. 2(a), "quantum good-cavity regime"] and for $\rho=1$, $\gamma=0$, and $\kappa=0.5,1,5$ [Fig. 2(b), "quantum superradiant regime"]. In the special case where atomic loss equals cavity loss (i.e., when $\gamma=\kappa$), $g=g^{(0)}-\gamma$, where $g^{(0)}$ is shown by dashed lines in Figs. 1 and 2.

Notice that g is asymmetric around $\delta=0$ in the "semiclassical regime," but symmetric around $\delta=1/\rho$ in the "quantum regime." This is a reflection of the different gain mechanism

in the two regimes: in the first case gain results from the difference between emission and absorption rates, as in the free-electron-laser gain [19]; on the contrary, in the quantum regime absorption is inhibited by the photon recoil shift and atoms behave as an inverted system, in a similar way as it occurs in a laser.

B. Average populations and number squeezing parameter

Figures 3 and 4 show the effect of losses in the semiclassical regime on the atomic population $\langle\hat{n}_1\rangle$ (a), and on the number squeezing parameter $\xi_{1,2}$ (b), plotted as a function of
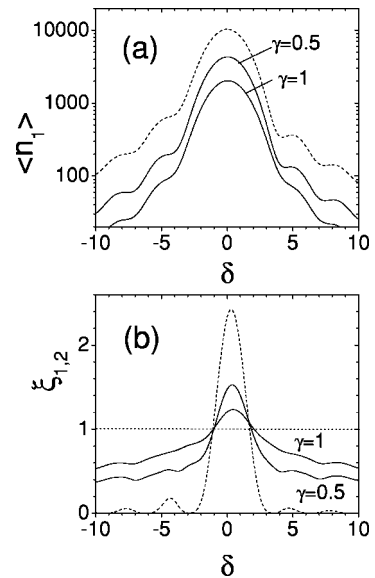

FIG. 3. Semiclassical regime with $\kappa=0$: (a) $\langle\hat{n}_1\rangle$ and (b) $\xi_{1,2}$ vs δ for $\rho=100$, $\tau=2$, $\gamma=0$ (dashed line), 0.5, and 1.
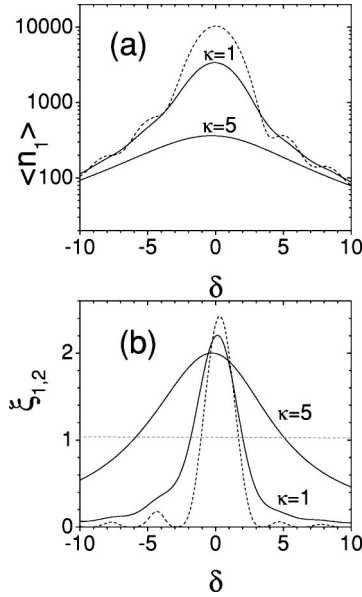
FIG. 4. Semiclassical regime with $\gamma=0$: (a) $\langle \hat{n}_1 \rangle$ and (b) $\xi_{1,2}$ vs δ for $\rho=100$, $\tau=2$, $\kappa=0$ (dashed line), 1, and 5.

δ for $\rho=100$ and $\tau=2$. Figure 3 shows the effect of the atomic decoherence on the high-Q cavity regime ($\kappa=0$) for $\gamma=0$ (dashed line), 0.5, and 1. We observe that increasing γ the population of the mode 1 decreases and the number squeezing parameter $\xi_{1,2}$ increases in the region of detuning where $\xi_{1,2}$ is less than unity, i.e., where atom-atom number squeezing occurs. A similar behavior is observed increasing the radiation losses in the semiclassical regime as shown in Fig. 4, where $\langle \hat{n}_1 \rangle$ (a) and $\xi_{1,2}$ (b) are plotted vs δ for $\gamma=0$, $\kappa=0,1,5$, and $\rho=100$. In both the cases, in order to observe number squeezing in the semiclassical regime, it is necessary to detune the probe field from resonance, as was already pointed out in Ref. [6].

Notice that the linear approximation of the CARL dynamics is justified until when the average populations $\langle \hat{n}_1 \rangle$ and $\langle \hat{n}_2 \rangle$ of the two "side-modes" remain much less than N, otherwise the depletion of the atomic pump mode must be taken into account and the nonlinear dynamics addressed. In our model the parameter N is imbedded in the dimensionless time $\tau=\omega_r \rho t$, where the CARL parameter ρ is proportional to $N^{1/3}$ [2].

The inclusion of losses also allows us to reach a steady-state regime when the gain g is negative. In this case, the covariance matrix $\mathbf{C}(\infty)=\mathbf{Q}(\infty)$ becomes asymptotically constant. An example of this behavior is shown in Fig. 5, where $\langle \hat{n}_1 \rangle$ (a) and $\xi_{1,2}$ (b) are plotted vs τ for $\rho=100$ and $\delta=3.5$. The dashed line shows the ideal case $\gamma=\kappa=0$: because $g^{(0)}=0$ (as can be observed from Fig. 1), the solution is oscillating and the two atomic modes 1 and 2 are periodically number squeezed. The dotted line of Fig. 5 shows the case with $\kappa=0$ and $\gamma=0.2$. Here, $g=0.025$ and both the average population and the number squeezing parameter grow in time. Finally, the continuous line of Fig. 5 shows the case $\gamma=\kappa=0.5$: the gain is $g=-0.5$ and the system reaches a stationary state in which $\xi_{1,2}=0.7$. This case is of some interest because a steady-state atom-atom number squeezed state is obtained in a linear system.
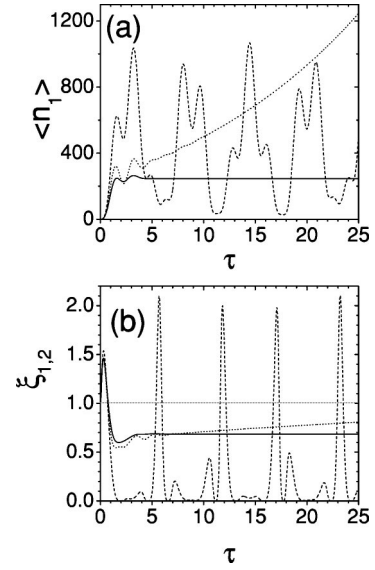

FIG. 5. Semiclassical regime for $\rho=100$ and $\delta=3.5$: (a) $\langle \hat{n}_1 \rangle$ and (b) $\xi_{1,2}$ vs τ for $\gamma=0$, $\kappa=0$ (dashed line), for $\gamma=0.2$, $\kappa=0$ (dotted line), and for $\gamma=\kappa=0.5$ (continuous line).

Let us now consider the effect of losses on the quantum regime. Figure 6 shows the average population $\langle \hat{n}_1 \rangle$ (a) and the atom-photon number squeezing parameter $\xi_{1,3}$ (b) as a function of τ for $1/\rho=\delta=5$. Dashed lines in Figs. 6(a) and 6(b) are for $\kappa=\gamma=0$, the dotted lines are for $\kappa=0$ and $\gamma=0.15$, and the continuous lines are for $\kappa=\gamma=0.15$. We note that the atomic decoherence (i.e., γ) causes a drastic reduction of the number squeezing between atoms and photons. However, choosing $\gamma=\kappa<g^{(0)}$ (where $g^{(0)}<\sqrt{\rho/2}$), we may keep $\xi_{1,3}$ constant and less than unity for a relatively long time, as in the ideal case without losses. Notice that in the quantum regime the below-threshold case (i.e., $g<\gamma$) is not of interest because the average number of quanta generated in each mode remains less than unity.
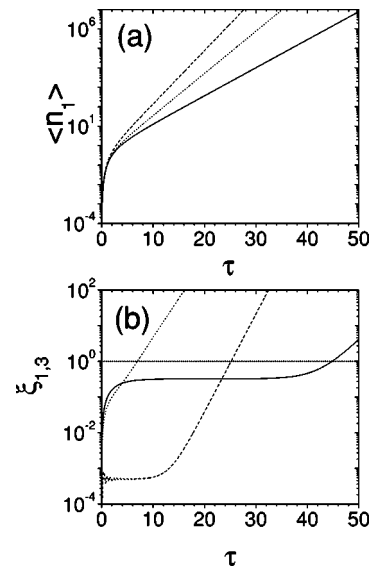

FIG. 6. Quantum regime for $1/\rho=\delta=5$: (a) $\langle \hat{n}_1 \rangle$ and (b) $\xi_{1,3}$ vs τ for $\gamma=0$, $\kappa=0$ (dashed line), for $\gamma=0.15$, $\kappa=0$ (dotted line), and for $\gamma=\kappa=0.15$ (continuous line).

C. Superradiant regime

In this section we present analytical results for the superradiant regime in the asymptotic limit $|\text{Im}\,\omega_1|\tau \gg 1$, where ω_1 is the unstable root of Eq. (28) with a negative imaginary part. For $\kappa \gg |\omega_1|$ and assuming for simplicity $\gamma=0$, one root of Eq. (28) can be discharged as it decays to zero as $\exp(-\kappa\tau)$ and the other two roots may be obtained solving the following quadratic equation:

$$\omega^2 + \frac{\omega + \delta + i\kappa}{(\delta + i\kappa)^2 - 1/\rho^2} - \frac{1}{\rho^2} = 0. \qquad (29)$$

From Eq. (29) it is possible to calculate explicitly the unstable root and evaluate asymptotically the expressions of the function f_{ij} appearing in Eq. (13). From them, it is possible to evaluate the expectation values of the occupation numbers in the semiclassical and quantum regimes.

1. Semiclassical limit of the superradiant regime

For $\kappa^{3/2} > 1 \gg \sqrt{\kappa}/\rho$ and $\delta=0$, the solutions of Eq. (29) are $\omega_{1,2} = \approx (1 \mp i)/\sqrt{2\kappa}$ and the average occupation numbers are

$$\langle \hat{n}_1 \rangle \approx \frac{\rho^2}{16\kappa}\left[1 + \frac{\sqrt{2\kappa}}{\rho}\right]e^{(2/\kappa)^{1/2}\tau}, \qquad (30)$$

$$\langle n_2 \rangle \approx \frac{\rho^2}{16\kappa}e^{(2/\kappa)^{1/2}\tau}, \qquad (31)$$

$$\langle n_3 \rangle \approx \frac{\rho}{8\kappa^2}e^{(2/\kappa)^{1/2}\tau}. \qquad (32)$$

We observe that the growth rate is proportional to $\sqrt{N}$ [17] and $\langle \hat{n}_1 \rangle \approx \langle \hat{n}_2 \rangle$ and $\langle \hat{n}_3 \rangle \approx (2/\rho\kappa)\langle \hat{n}_1 \rangle \ll \langle \hat{n}_1 \rangle$, so that the number of emitted photons is much smaller than the number of atoms in the two motional states. The asymptotic expression of the expectation value (27) of the bunching parameter is

$$\langle \hat{B}^\dagger \hat{B} \rangle \approx \frac{1}{4N}\left[1 + \frac{\sqrt{2\kappa}}{\rho}\right]e^{(2/\kappa)^{1/2}\tau}. \qquad (33)$$

Assuming that $\langle \hat{B}^\dagger \hat{B} \rangle$ approaches a maximum value of the order of 1, then the maximum average number of emitted photons is about $\rho N/2\kappa^2$, whereas the maximum fraction of atoms gaining a momentum $2\hbar k_p$ is about $\rho^2/4\kappa$.

2. Quantum limit of the superradiant regime

For $\kappa^{3/2} \gg 1 > \rho/\sqrt{\kappa}$ and $\delta=1/\rho$, the solutions of Eq. (29) are $\omega_{1,2} \approx 1/\rho \mp i\rho/(2\kappa)$ and the average occupation numbers are

$$\langle \hat{n}_1 \rangle \approx \left[1 + \left(\frac{\rho}{\sqrt{2\kappa}}\right)^4\right]e^{(\rho/\kappa)\tau}, \qquad (34)$$

$$\langle n_2 \rangle \approx \left(\frac{\rho}{2\sqrt{\kappa}}\right)^4 e^{(\rho/\kappa)\tau}, \qquad (35)$$

$$\langle n_3 \rangle \approx \frac{\rho}{2\kappa^2}e^{(\rho/\kappa)\tau}. \qquad (36)$$

In this case, the growth rate is proportional to N (as in the usual superradiance [18]) and $\langle \hat{n}_{2,3} \rangle \ll \langle \hat{n}_1 \rangle$ and $\langle \hat{n}_2 \rangle \approx (\rho/2)^3 \langle \hat{n}_3 \rangle$: the average number of emitted photons is much less than the average number of atoms scattering a photon from the pump to the probe. Furthermore, the number of atoms making the reverse process, i.e., scattering a photon from the probe to the pump, can be larger than the number of photons scattered into the probe mode if $\rho > 2$, as it occurs in the current experiment on BEC superradiance [7,9]. In this regime the asymptotic expression of the expectation value of the bunching parameter is

$$\langle \hat{B}^\dagger \hat{B} \rangle \approx \frac{1}{N}\left[1 + \frac{1}{2}\left(\frac{\rho}{\sqrt{2\kappa}}\right)^4\right]e^{(\rho/\kappa)\tau}, \qquad (37)$$

so that $\langle \hat{n}_3 \rangle \approx (\rho N/2\kappa^2)\langle \hat{B}^\dagger \hat{B} \rangle$, as in the semiclassical limit. The only difference is that in the quantum regime the maximum of $\langle \hat{B}^\dagger \hat{B} \rangle$ is $1/2$, so that the maximum number of scattered photons in the quantum limit is half of that obtained in the semiclassical limit.

V. ENTANGLEMENT AND SEPARABILITY

In this section we analyze the kind of entanglement that can be generated from our system. First, we establish notation and illustrate the separability criteria. We also apply the criteria to the state obtained in the ideal dynamics. Then, we address the effects of losses. We study both the separability properties of the tripartite state resulting from the evolution from the vacuum, as well as of the three two-mode states that are obtained by partial tracing over one of the modes. The basis of our analysis is that both the tripartite state and the partial traces are Gaussian states at any time. Therefore, we are able to fully characterize three-mode and two-mode entanglement as a function of the interaction parameters [20,21].

A. Three-mode entanglement

Concerning entanglement properties, three-mode states may be classified as follows [21].

Class 1. Fully inseparable states, i.e., not separable for any grouping of the modes.

Class 2. One-mode biseparable states, which are separable if two of the modes are grouped together, but inseparable with respect to the other groupings.

Class 3. Two-mode biseparable states, which are separable with respect to two of the three possible bipartite groupings but inseparable with respect to the third.

Class 4. Three-mode biseparable states, which are separable with respect to all three bipartite groupings, but cannot be written as a product state.

Class 5. Fully separable states, which can be written as a three-mode product state.

Separability properties are determined by the characteristic

function. In order to simplify the analysis we rewrite the characteristic function (7) in terms of the real variables $\mathbf{x}^T \equiv (x_1, x_2, x_3, y_1, y_2, y_3)$ with $\xi_j = 2^{-1/2}(y_j - ix_j)$, $j = 1, 2, 3$. We have

$$\chi(\mathbf{x}) = \exp\left\{-\frac{1}{4}\mathbf{x}^T \mathbf{V}\mathbf{x}\right\}, \tag{38}$$

where

$$\mathbf{V} = 2\boldsymbol{\Lambda}_0 \begin{pmatrix} \mathbf{A} & -\mathbf{B} \\ \mathbf{B} & \mathbf{A} \end{pmatrix} \boldsymbol{\Lambda}_0, \tag{39}$$

with $\boldsymbol{\Lambda}_0 = \text{diag}(-1, 1, 1, 1, 1, 1)$ and

$$\mathbf{A} = \text{Re } \mathbf{C}, \quad \mathbf{B} = \text{Im } \mathbf{C}, \tag{40}$$

and where we omitted the explicit time dependence of the matrices. The entanglement properties of the three-mode state are determined by the positivity of the matrices

$$\Gamma_j = \Lambda_j \mathbf{V}\Lambda_j - i\mathbf{J}, \quad j = 1, 2, 3$$

[21], where $\Lambda_1 = \text{diag}(1, 1, 1, -1, 1, 1)$, $\Lambda_2 = \text{diag}(1, 1, 1, 1, -1, 1)$, $\Lambda_3 = \text{diag}(1, 1, 1, 1, 1, -1)$, and $\mathbf{J}$ is the symplectic block matrix

$$\mathbf{J} = \begin{pmatrix} 0 & -\mathbf{I} \\ \mathbf{I} & 0 \end{pmatrix}, \tag{41}$$

$\mathbf{I}$ being the 3×3 identity matrix. The positivity of the matrix Γ_j indicates that the jth mode may be factorized from the other two. Therefore, we have that (i) if $\Gamma_j < 0$ $\forall j$ the state is in class 1; (ii) if only one of the Γ_j is positive the state is in class 2; (iii) if only two of the Γ_j are positive the state is in class 3; (iv) if $\Gamma_j > 0$, $\forall j$ then the state is either in class 4 or in class 5.

The covariance matrix $\mathbf{V}$ can be written as

$$\mathbf{V} = \begin{pmatrix} \mathcal{G} & -\mathcal{A} & -\mathcal{B} & 0 & \mathcal{D} & \mathcal{E} \\ -\mathcal{A} & \mathcal{H} & \mathcal{C} & \mathcal{D} & 0 & -\mathcal{F} \\ -\mathcal{B} & \mathcal{C} & \mathcal{I} & \mathcal{E} & \mathcal{F} & 0 \\ 0 & \mathcal{D} & \mathcal{E} & \mathcal{G} & \mathcal{A} & \mathcal{B} \\ \mathcal{D} & 0 & \mathcal{F} & \mathcal{A} & \mathcal{H} & \mathcal{C} \\ \mathcal{E} & -\mathcal{F} & 0 & \mathcal{B} & \mathcal{C} & \mathcal{I} \end{pmatrix}, \tag{42}$$

where

$$\mathcal{A} = 2 \text{ Re } C_{12}, \quad \mathcal{D} = 2 \text{ Im } C_{12}, \quad \mathcal{G} = 2\langle \hat{n}_1 \rangle + 1,$$

$$\mathcal{B} = 2 \text{ Re } C_{13}, \quad \mathcal{E} = 2 \text{ Im } C_{13}, \quad \mathcal{H} = 2\langle \hat{n}_2 \rangle + 1,$$

$$\mathcal{C} = 2 \text{ Re } C_{23}, \quad \mathcal{F} = 2 \text{ Im } C_{23}, \quad \mathcal{I} = 2\langle \hat{n}_3 \rangle + 1, \tag{43}$$

and the matrix elements C_{ij} are reported in Appendix B. Let us first consider the ideal case, when no losses are present. In this case we can prove analytically that the evolved state (3) is fully inseparable. In fact, we have that

$$\mathcal{A} = 2\sqrt{\langle \hat{n}_2 \rangle(1 + \langle \hat{n}_1 \rangle)}\cos \phi_2, \quad \mathcal{D} = 2\sqrt{\langle \hat{n}_2 \rangle(1 + \langle \hat{n}_1 \rangle)}\sin \phi_2,$$

$$\mathcal{B} = 2\sqrt{\langle \hat{n}_3 \rangle(1 + \langle \hat{n}_1 \rangle)}\cos \phi_3, \quad \mathcal{E} = 2\sqrt{\langle \hat{n}_3 \rangle(1 + \langle \hat{n}_1 \rangle)}\sin \phi_3,$$
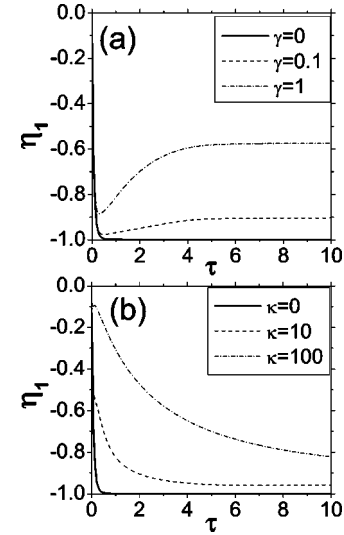

FIG. 7. Semiclassical regime for $\rho = 100$ and $\delta = 0.01$: minimum eigenvalue of matrix Γ_1 for $\kappa = 0$ and different values of γ (a) and for $\gamma = 0$ and different values of κ (b).

$$\mathcal{C} = 2\sqrt{\langle \hat{n}_2 \rangle\langle \hat{n}_3 \rangle}\cos(\phi_3 - \phi_2), \quad \mathcal{F} = 2\sqrt{\langle \hat{n}_2 \rangle\langle \hat{n}_3 \rangle}\sin(\phi_3 - \phi_2), \tag{44}$$

from which, in turn, it is straightforward to prove that the minimum eigenvalues of the matrices Γ_j are always negative. In the nonideal case, when γ or κ are different from zero, the expressions given in Eqs. (43) and accordingly the minimum eigenvalues of matrices Γ_j should be calculated numerically. In Figs. 7–9 the minimum eigenvalues of matrices Γ_1, Γ_2, and Γ_3 are plotted in the semiclassical regime, with $\rho = 100$. In this regime we can observe that modes 1 and 2 remain nonseparable from the three-mode state even for large values of atomic decoherence γ and radiation losses κ. Instead inseparability of mode 3 is not so robust especially in the pres-
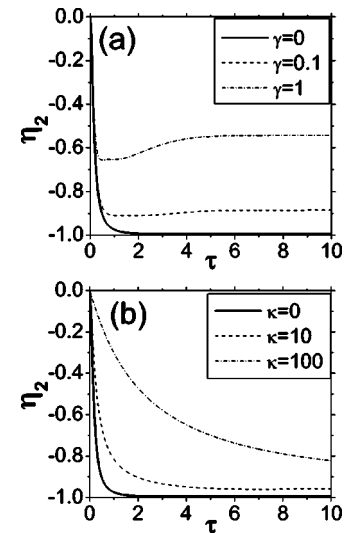

FIG. 8. Semiclassical regime for $\rho = 100$ and $\delta = 0.01$: minimum eigenvalue of matrix Γ_2 for $\kappa = 0$ and different values of γ (a) and for $\gamma = 0$ and different values of κ (b).
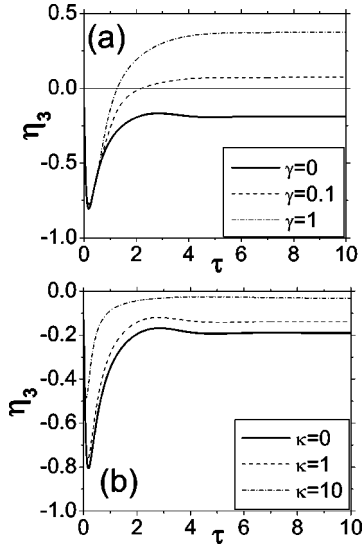
FIG. 9. Semiclassical regime for $\rho=100$ and $\delta=0.01$: minimum eigenvalue of matrix Γ_3 for $\kappa=0$ and different values of γ (a) and for $\gamma=0$ and different values of κ (b).

ence of some atomic decoherence. In Figs. 10 and 11 the minimum eigenvalues of matrices Γ_1 and Γ_2 are plotted in the quantum regime, with $\rho=0.2$. The minimum eigenvalue of the matrix Γ_3 is not reported in the figure since the behavior is similar to that of Γ_1. In this regime we can observe that modes 1 and 3 remain nonseparable from the three-mode state even for large values of atomic decoherence γ and radiation losses κ. Instead inseparability of mode 2 is very sensible, especially in the presence of some radiation losses. In any case in the quantum regime the three eigenvalues increasing γ and κ approach zero but remain negative.

B. Two-mode entanglement

In experimental conditions where only two of the modes are available for investigations, the relevant piece of infor-
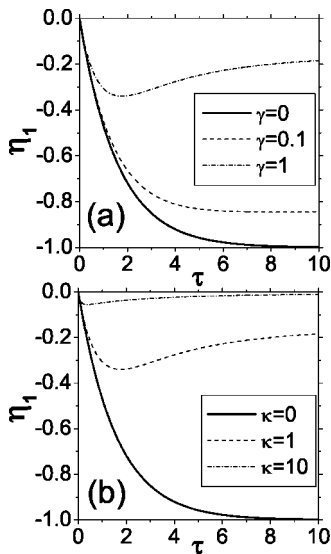

FIG. 10. Quantum regime for $\rho=0.2$ and $\delta=5$: minimum eigenvalue of matrix Γ_1 (or Γ_3, see the text) for $\kappa=0$ and different values of γ (a) and for $\gamma=0$ and different values of κ (b).
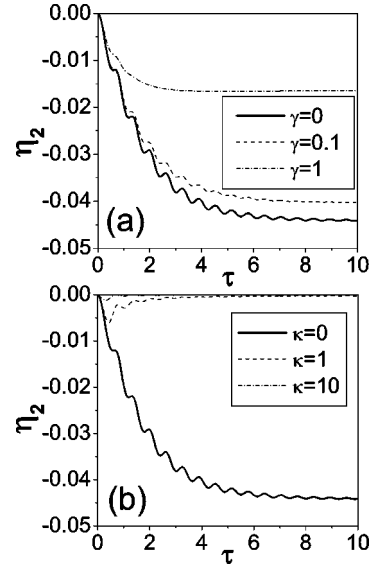

FIG. 11. Quantum regime for $\rho=0.2$ and $\delta=5$: minimum eigenvalue of matrix Γ_2 for $\kappa=0$ and different values of γ (a) and for $\gamma=0$ and different values of κ (b).

mation is contained in the partial traces of the global three-mode state. Therefore, besides the study of three-mode entanglement it is also of interest to analyze the two-mode entanglement properties of partial traces. At first we notice that the Gaussian character of the state is preserved by the partial trace operation. Moreover, the covariance matrices V_{ij} of three possible partial traces $\hat{\varrho}_{ij}=\mathrm{Tr}_k[\hat{\varrho}]$, $i \neq j \neq k$ can be obtained from $\mathbf{V}$ by deleting the corresponding k and $k+3$ rows and columns. The Gaussian character of the partial traces also permits us to check separability using the necessary and sufficient conditions introduced in Ref. [20], namely by the positivity of the matrices $\mathbf{S}_{ij}$ and $\mathbf{S}'_{ij}$ that are obtained by deleting the k and $k+3$ rows and columns either from Γ_i or Γ_j. Since they differ only for the sign of some off-diagonal elements it is easy to prove that they have the same eigenvalues. Therefore, we employ only $\mathbf{S}_{ij}$ in checking separability. The matrices $\mathbf{S}_{ij}$ are given by

$$\mathbf{S}_{12}=\begin{pmatrix} \mathcal{G} & -\mathcal{A} & i & \mathcal{D} \\ -\mathcal{A} & \mathcal{H} & -\mathcal{D} & i \\ -i & -\mathcal{D} & \mathcal{G} & -\mathcal{A} \\ \mathcal{D} & -i & -\mathcal{A} & \mathcal{H} \end{pmatrix}, \quad (45)$$

$$\mathbf{S}_{13}=\begin{pmatrix} \mathcal{G} & -\mathcal{B} & i & \mathcal{E} \\ -\mathcal{B} & \mathcal{L} & -\mathcal{E} & i \\ -i & -\mathcal{E} & \mathcal{G} & -\mathcal{B} \\ \mathcal{E} & -i & -\mathcal{B} & \mathcal{I} \end{pmatrix}, \quad (46)$$

$$\mathbf{S}_{23} = \begin{pmatrix} \mathcal{H} & \mathcal{C} & i & -\mathcal{F} \\ \mathcal{C} & \mathcal{L} & -\mathcal{L} & i \\ -i & -\mathcal{L} & \mathcal{H} & -\mathcal{C} \\ -\mathcal{F} & -i & -\mathcal{C} & \mathcal{I} \end{pmatrix}. \qquad (47)$$

In ideal conditions with $\gamma = \kappa = 0$ the minimum eigenvalues of $\mathbf{S}_{1k}$, $k=2,3$ are given by

$$\eta_{1k} = \langle \hat{n}_1 \rangle + \langle \hat{n}_k \rangle - \sqrt{4\langle \hat{n}_k \rangle + (\langle \hat{n}_1 \rangle + \langle \hat{n}_k \rangle)^2} \qquad (48)$$

and thus are always negative. On the contrary, the minimum eigenvalue of S_{23} is given by

$$\eta_{23} = 1 + \langle \hat{n}_1 \rangle + \sqrt{(1 + \langle \hat{n}_1 \rangle)^2 - 4\langle \hat{n}_k \rangle}, \qquad (49)$$

where $\langle \hat{n}_k \rangle = \max(\langle \hat{n}_2 \rangle, \langle \hat{n}_3 \rangle)$. Note that η_{23} is always positive. Therefore, after partial tracing we may have atom-atom entanglement (entanglement between mode a_1 and mode a_2) or scattered atom-radiation entanglement (entanglement between mode a_1 and mode a_3) but no entanglement between mode a_2 and mode a_3.

For $\tau \gg 1$ we know the asymptotic expressions for populations in the ideal case without losses [6], so we can obtain the stationary value of η_{1k} as

$$\eta_{1k} \approx - \frac{2\langle \hat{n}_k \rangle}{\langle \hat{n}_1 \rangle + \langle \hat{n}_k \rangle}. \qquad (50)$$

In the high-gain semiclassical regime ($\rho \gg 1$) [6],

$$\langle \hat{n}_1 \rangle \approx \frac{1}{18}\left[\frac{\rho^2}{2} + \rho\right]e^{\sqrt{3}\tau}, \qquad (51)$$

$$\langle \hat{n}_2 \rangle \approx \frac{\rho^2}{36}e^{\sqrt{3}\tau}, \qquad (52)$$

$$\langle \hat{n}_3 \rangle \approx \frac{\rho}{18}e^{\sqrt{3}\tau}, \qquad (53)$$

so that

$$\eta_{12} \approx -\frac{\rho}{1+\rho}, \qquad \eta_{13} \approx -\frac{4}{4+\rho}. \qquad (54)$$

In the high-gain quantum regime ($\rho < 1$),

$$\langle n_1 \rangle \approx \frac{1}{4}\left[1 + \left(\frac{\rho}{2}\right)^3\right]e^{\sqrt{2\rho}\tau}, \qquad (55)$$

$$\langle n_2 \rangle \approx \frac{1}{4}\left(\frac{\rho}{2}\right)^3 e^{\sqrt{2\rho}\tau}, \qquad (56)$$

$$\langle n_3 \rangle \approx \frac{1}{4}e^{\sqrt{2\rho}\tau}, \qquad (57)$$

so that

$$\eta_{12} \approx -\frac{\rho^3}{4+\rho^3}, \qquad \eta_{13} \approx -\frac{16}{16+\rho^3}. \qquad (58)$$

In the nonideal case, when γ or κ are different from zero, the minimum eigenvalues of matrices S_{12} and S_{13} can be easily
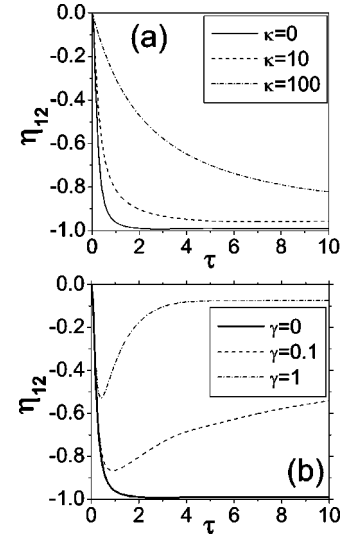

FIG. 12. Semiclassical regime for $\rho = 100$ and $\delta = 0$: minimum eigenvalue of matrix S_{12} for $\kappa = 0$ and different values of γ (a) and for $\gamma = 0$ and different values of κ (b).

obtained numerically. In Figs. 12 and 13 the minimum eigenvalues of matrices S_{12}, S_{13} are plotted for the semiclassical regime. We can observe that the atom-atom entanglement of the reduced state 12 is robust, as the minimum eigenvalue remains negative, increasing atomic decoherence γ and radiation losses κ. On the contrary, atom-photon entanglement of the reduced state 13 is more sensitive to noise: the eigenvalue remains negative increasing κ and becomes positive in the presence of some atomic decoherence.

In Figs. 14 and 15 are plotted the minimum eigenvalues of matrices S_{12}, S_{13} in the quantum regime, with $\rho = 0.2$. Here the atom-photon entanglement in the state 13 is robust while atom-atom entanglement of the state 12 is not. The minimum eigenvalue always remains negative, but it starts from a very small absolute value and approaches very fast to zero, increasing κ and γ.
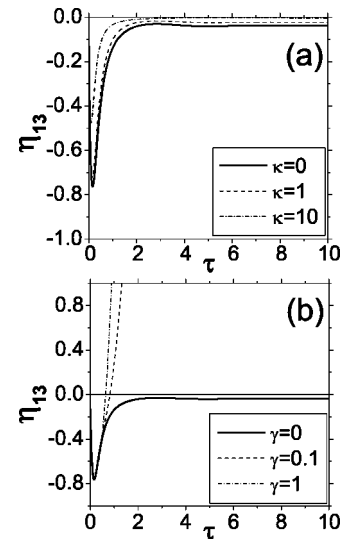

FIG. 13. Semiclassical regime for $\rho = 100$ and $\delta = 0$: minimum eigenvalue of matrix S_{13} for $\kappa = 0$ and different values of γ (a) and for $\gamma = 0$ and different values of κ (b).
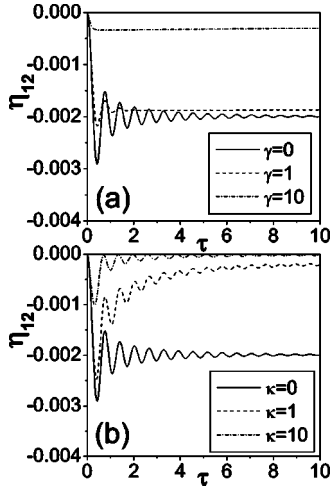
FIG. 14. Quantum regime for $\rho=0.2$ and $\delta=5$: minimum eigenvalue of matrix S_{12} for $\kappa=0$ and different values of γ (a) and for $\gamma=0$ and different values of κ (b).

VI. CONCLUSIONS

We have investigated how cavity radiation losses and atomic decoherence influence the generation of two- (atom-atom or atom-radiation) and three-mode entanglements in the collective atomic recoil lasing (CARL) by a Bose-Einstein condensate driven by a far off-resonant pump laser. The atoms backscatter photons from the pump to a weak radiation mode circulating in a ring cavity, recoiling with opposite momentum $\pm 2\hbar k_p$ along the ring cavity axis. Our analysis has been focused to the linear regime, in which the ground state of the condensate remains approximately undepleted and the dynamics is described by three parametrically coupled boson operators, corresponding to the radiation

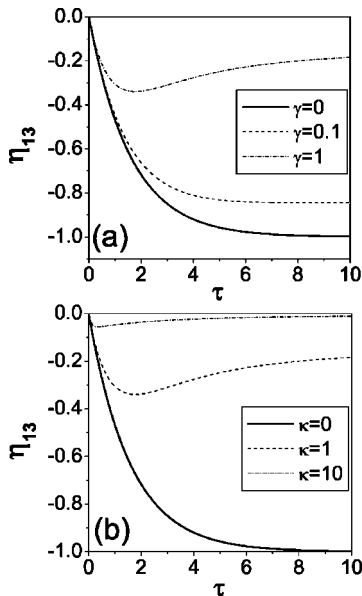

FIG. 15. Quantum regime for $\rho=0.2$ and $\delta=5$: minimum eigenvalue of matrix S_{13} for $\kappa=0$ and different values of γ (a) and for $\gamma=0$ and different values of κ (b).

mode and two condensates with momentum displaced by $\pm 2\hbar \vec{k}_p$. The problem resembles that of three optical modes generated in a $\chi^{(2)}$ medium [22] and thus our results may have a more general interest also behind the physics of the BEC. We have solved analytically the dissipative Master equation in terms of the Wigner function and we have investigated the entanglement properties of the evolved state. We found that three-mode entanglement as well as the two-mode atom-atom and atom-photon entanglements are generally robust against cavity losses and decoherence. Our analysis has been focused on the different dynamical regimes, the high-Q cavity regime, with low cavity losses, and the superradiant regime in the so-called "bad-cavity limit." We have found that entanglement in the high-Q cavity regime is generally robust against either cavity or decoherence losses. On the contrary, losses seriously limit atom-atom and atom-radiation number squeezing production in CARL [15], the only exception being the symmetric loss case $\gamma=\kappa$. Concerning the superradiant regime, atom-atom entanglement in the semiclassical limit is generally more robust than atom-radiation entanglement in the quantum limit. Finally, we have proved that the state generated in the ideal case without losses is fully inseparable. We conclude that the present system is a good candidate for the experimental observation of entanglement in condensate systems since, in particular, steady-state entanglement may be obtained both between atoms with opposite momenta and between atoms and photons. The main implications for CARL are twofold: on one hand the characterization of entanglement may be performed also in nonideal cases. On the other hand, the experimental requirements to implement the interspecies teleportation of Ref. [14] can be weakened without losing the nonlocal character of the protocol. It should also be mentioned that the separability criteria used here, i.e., the negativity of the modified covariance matrix, is related to the negativity of the partially transposed density matrix, which itself is a good measure of entanglement [23,24]. Therefore the present analysis, besides establishing a threshold for separability, also provides criteria to compare different working regimes in terms of the degree of entanglement.

APPENDIX A: SOLUTION OF THE FOKKER-PLANCK EQUATION

In order to solve Eq. (8) for the Green function $G(\mathbf{u},t;\mathbf{u}_0,0)$ it is helpful to first perform a similarity transformation to diagonalize the drift matrix $\mathbf{A}$:

$$\tilde{\mathbf{A}} = \mathbf{S}\mathbf{A}\mathbf{S}^{-1} = \text{diag}\{\lambda_1\lambda_2\lambda_3\}, \tag{A1}$$

where the complex eigenvalues λ_j of $\mathbf{A}$ (with $j=1,2,3$) are obtained from the characteristic equation

$$\det(\mathbf{A} - \lambda\mathbf{I}) = 0, \tag{A2}$$

$\mathbf{I}$ is the 3×3 identity matrix and the columns of $\mathbf{S}^{-1}$ are the right eigenvectors of $\mathbf{A}$ with $\det(\mathbf{S})=1$. Solving Eq. (A2) we obtain $\lambda_j = i(\omega_j - \delta) - \gamma_+$, where ω_j are the three roots of the cubic equation (15), whereas the eigenvectors of $\mathbf{A}$ corresponding to the jth eigenvalue are

$$\mathbf{a}_j^T = \mathcal{N}_j\left(i\sqrt{\frac{\rho}{2}}(\omega_j + \beta), -i\sqrt{\frac{\rho}{2}}(\omega_j - \beta), -\omega_j^2 + \beta^2\right), \tag{A3}$$

where $\beta = 1/\rho + i\gamma_-$ and

$$\mathcal{N}_1 = \frac{1}{\omega_2 - \omega_3}, \quad \mathcal{N}_2 = \frac{1}{\omega_1 - \omega_3}, \quad \mathcal{N}_3 = \frac{1}{\omega_1 - \omega_2}. \tag{A4}$$

Explicitly calculating the inverse matrix of S^{-1} we have

$$\mathbf{S} = \begin{pmatrix} i\sqrt{\rho/2}(a_{22}a_{23}/\mathcal{N}_1) & i\sqrt{\rho/2}(a_{12}a_{13}/\mathcal{N}_1) & -\mathcal{N}_2\mathcal{N}_3/\mathcal{N}_1 \\ -i\sqrt{\rho/2}(a_{23}a_{21}/\mathcal{N}_2) & -i\sqrt{\rho/2}(a_{11}a_{13}/\mathcal{N}_2) & \mathcal{N}_1\mathcal{N}_3/\mathcal{N}_2 \\ i\sqrt{\rho/2}(a_{21}a_{22}/\mathcal{N}_3) & i\sqrt{\rho/2}(a_{12}a_{11}/\mathcal{N}_3) & -\mathcal{N}_1\mathcal{N}_2/\mathcal{N}_3 \end{pmatrix}, \tag{A5}$$

where $a_{ij}=(\mathbf{a}_j)_i$. Now we transform the Fokker-Plank equation (8) in the new variable $\mathbf{v}\equiv\mathbf{S}\mathbf{u}$. From Eq. (A1) we obtain

$$\mathbf{u}'^T\mathbf{A}\mathbf{u} = \mathbf{u}'^T(\mathbf{S}^{-1}\tilde{\mathbf{A}}\mathbf{S})\mathbf{u} = \mathbf{v}'^T\tilde{\mathbf{A}}\mathbf{v}, \tag{A6}$$

$$\mathbf{u}'^T\mathbf{D}\mathbf{u}'^* = (\mathbf{v}'^T\mathbf{S})\mathbf{D}(\mathbf{S}^T\mathbf{v}')^* = \mathbf{v}'^T\tilde{\mathbf{D}}\mathbf{v}'^*, \tag{A7}$$

where $\tilde{\mathbf{D}}\equiv\mathbf{S}\mathbf{D}\mathbf{S}^\dagger$, $\mathbf{S}^\dagger=(\mathbf{S}^T)^*$, and $\mathbf{v}'^T=\mathbf{u}'^T\mathbf{S}^{-1}$. Using Eqs. (A6) and (A7) Eq. (8) becomes

$$\frac{\partial\tilde{W}}{\partial\tau} = -(\mathbf{v}'^T\tilde{\mathbf{A}}\mathbf{v} + \text{c.c.})\tilde{W} + \mathbf{v}'^T\tilde{\mathbf{D}}\mathbf{v}'^*\tilde{W}, \tag{A8}$$

where $\tilde{W}(\mathbf{v},\tau)=W(\mathbf{S}^{-1}\mathbf{v},\tau)$. Equation (A8) is a linear Fokker-Planck equation with diagonal drift. Introducing the Fourier transform

$$\tilde{U}(\mathbf{k},\tau) = \int\frac{d^2\mathbf{k}}{\pi^3}\tilde{W}(\mathbf{v})\exp(\mathbf{k}^{*T}\mathbf{v} - \mathbf{k}^T\mathbf{v}^*), \tag{A9}$$

Eq. (A8) becomes

$$\frac{\partial\tilde{U}}{\partial\tau} = (\mathbf{k}^{*T}\tilde{\mathbf{A}}\mathbf{k}'^* + \mathbf{k}^T\tilde{\mathbf{A}}^*\mathbf{k}')\tilde{U} - (\mathbf{k}^{*T}\tilde{\mathbf{D}}\mathbf{k})\tilde{U}, \tag{A10}$$

where

$$\mathbf{k}^T = (k_1,k_2,k_3), \quad \mathbf{k}'^T = \left(\frac{\partial}{\partial k_1},\frac{\partial}{\partial k_2},\frac{\partial}{\partial k_3}\right). \tag{A11}$$

The Fourier transform of the initial condition of the Green function $\tilde{G}(\mathbf{v},0;\mathbf{S}\mathbf{u}_0,0)=\delta^3(\mathbf{v}-\mathbf{S}\mathbf{u}_0)$ is

$$\tilde{U}(\mathbf{k},0) = \exp[\mathbf{k}^{*T}\mathbf{S}\mathbf{u}_0 - \mathbf{k}^T(\mathbf{S}\mathbf{u}_0)^*]. \tag{A12}$$

Equation (A10) is now solved using the method of the characteristics. Since $\tilde{\mathbf{A}}$ is diagonal the subsidiary equations are

$$\frac{d\tau}{1} = \frac{dk_1^*}{-\lambda_1 k_2^*} = \frac{dk_2^*}{-\lambda_2 k_2^*} = \frac{dk_3^*}{-\lambda_3 k_3^*} = \frac{d\tilde{U}}{(-\mathbf{k}^{*T}\tilde{\mathbf{D}}\mathbf{k})\tilde{U}} \tag{A13}$$

and have solutions

$$\mathbf{k} = e^{-\tilde{\mathbf{A}}^*\tau}\mathbf{c} = \text{const.} \tag{A14}$$

Then

$$\frac{d\tilde{U}}{\tilde{U}} = -\mathbf{k}^{*T}\tilde{\mathbf{D}}\mathbf{k}d\tau = -\mathbf{c}^{*T}(e^{-\tilde{\mathbf{A}}}\tilde{\mathbf{D}}e^{-\tilde{\mathbf{A}}^*\tau})\mathbf{c}d\tau =$$

$$-\mathbf{c}^{*T}[\tilde{\mathbf{D}}_{ij}e^{-(\lambda_i+\lambda_j^*)\tau}]\mathbf{c}d\tau, \tag{A15}$$

where $(\mathbf{B}_{ij})$ denotes the matrix with elements $\mathbf{B}_{ij}$, and we find, using Eq. (A14),

$$\ln\tilde{U} = \mathbf{k}^{*T}\left\{\frac{\tilde{\mathbf{D}}_{ij}}{\lambda_i + \lambda_j^*}[1 - e^{(\lambda_i+\lambda_j^*)\tau}]\right\}\mathbf{k} + \text{const.} \tag{A16}$$

It follows that

$$\tilde{U}\exp\{\mathbf{k}^{*T}\tilde{\mathbf{Q}}\mathbf{k}\} = \text{const}, \tag{A17}$$

where $\tilde{\mathbf{Q}}$ is the 3×3 matrix with elements

$$\tilde{Q}_{ij} \equiv -\frac{\tilde{D}_{ij}}{\lambda_i + \lambda_j^*}[1 - e^{(\lambda_i+\lambda_j^*)\tau}] = \int_0^\tau d\tau'\tilde{D}_{ij}e^{(\lambda_i+\lambda_j^*)\tau'}. \tag{A18}$$

Thus, from Eqs. (A14) and (A17), the solution for $\tilde{U}$ takes the general form

$$\tilde{U}(\mathbf{k},\tau) = \Phi(e^{\tilde{\mathbf{A}}^*\tau}\mathbf{k})\exp\{-\mathbf{k}^{*T}\tilde{\mathbf{Q}}\mathbf{k}\}, \tag{A19}$$

where Φ is an arbitrary function. Choosing Φ to match the initial condition (A12), we find

$$\widetilde{U}(\mathbf{k},\tau) = \exp\{\mathbf{k}^{*T}(\mathbf{S}e^{\mathbf{A}\tau}\mathbf{u}_0) - \mathbf{k}^T(\mathbf{S}e^{\mathbf{A}\tau}\mathbf{u}_0)^*\}\exp\{-\mathbf{k}^{*T}\widetilde{\mathbf{Q}}k\}. \tag{A20}$$

In the argument of the first exponential on the right-hand side we have used Eq. (A1) to write $\exp(\widetilde{\mathbf{A}}\tau)\mathbf{S}=\mathbf{S}\exp(\mathbf{A}\tau)$. Inverting the Fourier transform we obtain

$$\widetilde{G}(\mathbf{v},\tau;\mathbf{S}\mathbf{u}_0,0) = \frac{1}{\pi^3\det\widetilde{\mathbf{Q}}}\exp\{(\mathbf{v}-\mathbf{S}e^{\mathbf{A}\tau}\mathbf{u}_0)^\dagger\widetilde{\mathbf{Q}}^{-1}(\mathbf{v}-\mathbf{S}e^{\widetilde{\mathbf{A}}\tau}\mathbf{u}_0)\} \tag{A21}$$

and so transforming back the variables

$$G(\mathbf{u},\tau;\mathbf{u}_0,0) = \frac{1}{\pi^3\det\mathbf{Q}}\exp\{(\mathbf{u}-e^{\mathbf{A}\tau}\mathbf{u}_0)^\dagger\mathbf{Q}^{-1}(\mathbf{u}-e^{\mathbf{A}\tau}\mathbf{u}_0)\}, \tag{A22}$$

where

$$\mathbf{Q} = \mathbf{S}^{-1}\hat{\mathbf{Q}}(\mathbf{S}^{-1})^\dagger = \int_0^\tau d\tau' e^{\mathbf{A}\tau'}\mathbf{D}(e^{\mathbf{A}\tau'})^\dagger. \tag{A23}$$

APPENDIX B: ELEMENTS OF THE MATRICES M, EQ. (13), AND C, EQ. (18)

The expressions of the functions f_{ij} which appear as elements of the matrix **M**, Eq. (13), are

$$f_{11}(\tau) = e^{-(\gamma_+ + i\delta)\tau}\sum_{j=1}^3 [(\omega_j-\alpha)(\omega_j+\beta)-\rho/2]\frac{e^{i\omega_j\tau}}{\Delta_j}, \tag{B1}$$

$$f_{22}(\tau) = e^{-(\gamma_+ + i\delta)\tau}\sum_{j=1}^3 [(\omega_j-\alpha)(\omega_j-\beta)+\rho/2]\frac{e^{i\omega_j\tau}}{\Delta_j}, \tag{B2}$$

$$f_{33}(\tau) = e^{-(\gamma_+ + i\delta)\tau}\sum_{j=1}^3 (\omega_j^2-\beta^2)\frac{e^{i\omega_j\tau}}{\Delta_j}, \tag{B3}$$

$$f_{12}(\tau) = -\frac{\rho}{2}e^{-(\gamma_+ + i\delta)\tau}\sum_{j=1}^3 \frac{e^{i\omega_j\tau}}{\Delta_j}, \tag{B4}$$

$$f_{13}(\tau) = -i\sqrt{\frac{\rho}{2}}e^{-(\gamma_+ + i\delta)\tau}\sum_{j=1}^3 (\omega_j+\beta)\frac{e^{i\omega_j\tau}}{\Delta_j}, \tag{B5}$$

$$f_{23}(\tau) = i\sqrt{\frac{\rho}{2}}e^{-(\gamma_+ + i\delta)\tau}\sum_{j=1}^3 (\omega_j-\beta)\frac{e^{i\omega_j\tau}}{\Delta_j}, \tag{B6}$$

where $\alpha=\delta+i(\kappa-\gamma_+)$, $\beta=1/\rho+i\gamma_-$, $\Delta_j=(\omega_j-\omega_k)(\omega_j-\omega_m)$ (with $j\neq k\neq m$), and ω_1, ω_2, and ω_3 are the roots of the cubic equation (15). It is possible to show that $f_{ij}(0)=\delta_{ij}$ in order to satisfy the initial condition $\mathbf{M}(0)=\mathbf{I}$.

The explicit components of the covariance matrix

$$\mathbf{C}(\tau) = \mathbf{Q}(\tau) + \frac{1}{2}\mathbf{M}(\tau)\mathbf{M}^\dagger(\tau), \tag{B7}$$

where **M** and **Q** are defined in Eqs. (13) and (14), are

$$C_{11}(\tau) = \int_0^\tau d\tau'\{\gamma_1|f_{11}|^2 + \gamma_2|f_{12}|^2 + \kappa|f_{13}|^2\} + \frac{1}{2}(|f_{11}|^2 + |f_{12}|^2 + |f_{13}|^2), \tag{B8}$$

$$C_{22}(\tau) = \int_0^\tau d\tau'\{\gamma_1|f_{12}|^2 + \gamma_2|f_{22}|^2 + \kappa|f_{23}|^2\} + \frac{1}{2}(|f_{12}|^2 + |f_{22}|^2 + |f_{23}|^2), \tag{B9}$$

$$C_{33}(\tau) = \int_0^\tau d\tau'\{\gamma_1|f_{13}|^2 + \gamma_2|f_{23}|^2 + \kappa|f_{33}|^2\} + \frac{1}{2}(|f_{13}|^2 + |f_{23}|^2 + |f_{33}|^2), \tag{B10}$$

$$C_{12}(\tau) = \int_0^\tau d\tau'\{-\gamma_1 f_{11}f_{12}^* + \gamma_2 f_{12}f_{22}^* + \kappa f_{13}f_{23}^*\} + \frac{1}{2}(-f_{11}f_{12}^* + f_{12}f_{22}^* + f_{13}f_{23}^*), \tag{B11}$$

$$C_{13}(\tau) = \int_0^\tau d\tau'\{\gamma_1 f_{11}f_{13}^* - \gamma_2 f_{12}f_{23}^* + \kappa f_{13}f_{33}^*\} + \frac{1}{2}(f_{11}f_{13}^* - f_{12}f_{23}^* + f_{13}f_{33}^*), \tag{B12}$$

$$C_{23}(\tau) = \int_0^\tau d\tau'\{-\gamma_1 f_{12}f_{13}^* - \gamma_2 f_{22}f_{23}^* + \kappa f_{23}f_{33}^*\} + \frac{1}{2}(-f_{12}f_{13}^* - f_{22}f_{23}^* + f_{23}f_{33}^*), \tag{B13}$$

with $C_{ij}=C_{ji}^*$.

In the special case $\gamma_+=\gamma=\kappa$ and $\gamma_-=0$, $f_{ij}=e^{-\gamma\tau}f_{ij}^{(0)}$, where $f_{ij}^{(0)}$ is the solution without losses. As shown in Ref. [6], they satisfy the following relations:

$$|f_{13}^{(0)}|^2 + 1 = |f_{23}^{(0)}|^2 + |f_{33}^{(0)}|^2, \tag{B14}$$

$$|f_{11}^{(0)}|^2 - 1 = |f_{12}^{(0)}|^2 + |f_{13}^{(0)}|^2, \tag{B15}$$

$$|f_{12}^{(0)}|^2 + 1 = |f_{22}^{(0)}|^2 + |f_{23}^{(0)}|^2, \tag{B16}$$

$$f_{11}^{(0)}(f_{13}^{(0)})^* = -f_{12}^{(0)}(f_{23}^{(0)})^* + f_{13}^{(0)}(f_{33}^{(0)})^*, \tag{B17}$$

$$-f_{11}^{(0)}(f_{12}^{(0)})^* = f_{12}^{(0)}(f_{22}^{(0)})^* + f_{13}^{(0)}(f_{23}^{(0)})^*, \tag{B18}$$

$$-f_{12}^{(0)}(f_{13}^{(0)})^* = -f_{22}^{(0)}(f_{23}^{(0)})^* + f_{23}^{(0)}(f_{33}^{(0)})^*. \quad \text{(B19)}$$

Using Eqs. (B14)–(B16) in Eqs. (B8)–(B10) and $C_{ii}=1/2 +\langle\hat{n}_i\rangle$, we obtain that

$$\langle\hat{n}_1\rangle = \langle\hat{n}_2\rangle + \langle\hat{n}_3\rangle \quad \text{(B20)}$$

and

$$\frac{d\langle\hat{n}_i\rangle}{d\tau} = \frac{d\langle\hat{n}_i^{(0)}\rangle}{d\tau}e^{-2\gamma\tau}, \quad \text{(B21)}$$

where $\langle\hat{n}_i^{(0)}\rangle$ are the expectation values of the occupation numbers of the three modes in the ideal case without losses.

[1] P. Meystre, *Atom Optics* (Springer, Berlin, 2001).

[2] R. Bonifacio and L. De Salvo Souza, Nucl. Instrum. Methods Phys. Res. A **341**, 360 (1994); R. Bonifacio, L. De Salvo Souza, L. M. Narducci, and E. J. D'Angelo, Phys. Rev. A **50**, 1716 (1994).

[3] R. Bonifacio, Opt. Commun. **146**, 236 (1998).

[4] M. G. Moore and P. Meystre, Phys. Rev. A **58**, 3248 (1998).

[5] M. G. Moore, O. Zobay, and P. Meystre, Phys. Rev. A **60**, 1491 (1999).

[6] N. Piovella, M. Cola, and R. Bonifacio, Phys. Rev. A **67**, 013817 (2003).

[7] S. Inouye, A. P. Chikkatur, D. M. Stamper-Kurn, J. Stenger, D. E. Pritchard, and W. Ketterle, Science **285**, 571 (1999).

[8] M. Kozuma, Y. Suzuki, Y. Torii, T. Sugiura, T. Kugam, E. W. Hagley, and L. Deng, Science **286**, 2309 (1999).

[9] R. Bonifacio, F. S. Cataliotti, M. Cola, L. Fallani, C. Fort, N. Piovella, and M. Inguscio, Opt. Commun. **233**, 155 (2004).

[10] M. G. Moore and P. Meystre, Phys. Rev. Lett. **83**, 5202 (1999).

[11] D. Kruse, C. von Cube, C. Zimmermann, and P. Courteille, Phys. Rev. Lett. **91**, 183601 (2003).

[12] T. Gasenzer, D. C. Roberts, and K. Burnett, Phys. Rev. A **65**, 021605(R) (2002).

[13] D. Deb and G. S. Agarwal, Phys. Rev. A **65**, 063618 (2002).

[14] M. G. A. Paris, M. Cola, N. Piovella, and R. Bonifacio, Opt. Commun. **227**, 349 (2003).

[15] T. Gasenzer, J. Phys. B **35**, 2337 (2002).

[16] H. J. Carmichael, *Statistical Methods in Quantum Optics 1* (Springer, Berlin, 1999).

[17] N. Piovella, M. Gatelli, and R. Bonifacio, Opt. Commun. **194**, 167 (2001).

[18] R. Bonifacio, P. Schwendimann, and F. Haake, Phys. Rev. A **4**, 302 (1971).

[19] J. M. J. Madey, J. Appl. Phys. **42**, 1906 (1971).

[20] R. Simon, Phys. Rev. Lett. **84**, 2726 (2000).

[21] G. Giedke, B. Kraus, M. Lewenstein, and J. I. Cirac, Phys. Rev. A **64**, 052303 (2001).

[22] A. Allevi *et al.*, Opt. Lett. **29**, 180 (2004); J. Mod. Opt. **51**, 1031 (2004); A. Ferraro *et al.*, J. Opt. Soc. Am. B **21**, 1241 (2004).

[23] G. Vidal and R. F. Werner, Phys. Rev. A **65**, 032314 (2002).

[24] J. Eisert, C. Simon, and M. B. Plenio, J. Phys. A **35**, 3911 (2002).